ACCELERATED THRESHOLD FATIGUE CRACK GROWTH EFFECT – POWDER METALLURGY ALUMINUM ALLOY

R. S. Piascik* and J. A. Newman†

Fatigue crack growth (FCG) research conducted in the near threshold regime has identified a room temperature creep crack growth damage mechanism for a fine grain powder metallurgy (PM) aluminum alloy (8009). At very low ΔK, an abrupt acceleration in room temperature FCG rate occurs at high stress ratio ($R = K_{min}/K_{max}$). The near threshold accelerated FCG rates are exacerbated by increased levels of K_{max} ($K_{max} \geq 0.4\ K_{IC}$). Detailed fractographic analysis correlates accelerated FCG with the formation of crack-tip process zone micro-void damage. Experimental results show that the near threshold and K_{max} influenced accelerated crack growth is time and temperature dependent.

INTRODUCTION

In cases where fatigue lives primarily depend on the early stages of crack growth, it is critical to understand the FCG characteristics in the near threshold regime, defined schematically in Figure 1. Considerable research has shown that an acceleration in near threshold FCG rates (d*a*/dN) occurs with increasing stress ratio due to a reduction in crack closure (Newman and Elber [1]). However, research has suggested that crack closure does not account for all stress ratio effects when R ranges from 0.5 to 0.95, and for K_{max} greater than 0.4 K_{IC} (Gan and Weertman [2] and Beevers [3]). This work suggests that near threshold FCG can be influenced by other crack-tip damage mechanisms (K_{max} effects) that are not related to crack closure. For ingot metallurgy aluminum and titanium alloys, relatively small near threshold K_{max} effects have been observed during closure free FCG [3]. Others have concluded that highly accelerated near threshold FCG rates during constant-K_{max} testing of low toughness titanium and nickel-based alloys are due to hydrogen assisted cracking (Marci [4] and Lang, et al. [5, 6]).

* NASA Langley Research Center, Metals and Thermal Structures Branch, MS 188E, Hampton, VA 23681, USA.

† U.S. Army Research Laboratory, Vehicle Technology Directorate, MS 188E, Hampton, VA 23681, USA.

The unusual room temperature near-threshold FCG behavior observed during constant-K_{max} testing (5.5 and 11 MPa$\sqrt{m}$) of a powder metallurgy (PM) aluminum alloy (8009) is plotted in Figure 2a (Newman [7]). Transitions to accelerated FCG rates (dramatic slope changes in the d*a*/dN versus ΔK data identified with arrows) were correlated with changes in crack surface morphology. For both levels of K_{max}, a flat fatigue crack surface morphology (micrographs shown in Figures 2c and 2e) was observed at higher levels of ΔK. As ΔK was reduced and accelerated d*a*/dN was observed, the fatigue crack surface abruptly changed to a micro-void morphology (shown in Figures 2b and 2d) similar to that observed during elevated temperature creep crack growth (Jata, et al. [8] and Claeys, et al. [9]). The aim of this research is to identify the near threshold crack-tip mechanisms that result in accelerated fatigue crack growth at room temperature.

EXPERIMENTAL PROCEDURES

Fatigue crack growth testing was conducted using aluminum alloy 8009; a powder-metallurgy (PM) dispersion-strengthened alloy that was developed to retain high strength at elevated temperatures. The nominal composition of alloy 8009 is 8.5^{w}/o-Fe, 1.3^{w}/o-V, and 1.7^{w}/o-Si [8, 9]. This alloy has an extremely fine microstructure with an average grain size for the matrix of approximately 500 nm. $Al_{12}(Fe,V)_3Si$ dispersoids comprise 25 volume percent of the alloy and range in size from 40nm to 80 nm.

Constant-K_{max} fatigue crack growth tests were conducted in laboratory air, and ΔK was reduced at a K-gradient of $C = -787\ m^{-1}$ (ASTM standards [10]). All tests were conducted using a computer-controlled servo-hydraulic test machine and the K-controlled tests were performed using the ASTM eccentrically-loaded-single-edge-notch tension ESE(T) specimen. Specimens having a width and thickness of 38.1 mm and 2.3 mm, respectively, were fabricated from 8009 aluminum sheet (Piascik, et al. [11]). The back-face strain compliance method was used to continuously monitor crack length. During the constant-K_{max} tests, K_{max} was held constant and increasing K_{min} and R was used to reduce ΔK. This test procedure was used so that FCG threshold conditions were achieved at high R, thus eliminating the affects of crack closure (Donald, et al. [12]). Constant ΔK tests were conducted to determine the affect of loading frequency on FCG. Under constant ΔK conditions, the plot of crack length versus load cycles was used to accurately determine the influence of frequency on d*a*/dN. FCG testing in ultrahigh vacuum (UHV) was conducted in a stainless steel chamber capable of a $1.3x10^{-7}$ Pa vacuum environment.

EXPERIMENTAL RESULTS AND DISCUSSION

Figure 3a shows the near threshold FCG characteristics in UHV at a constant K_{max} = 7.7 MPa√m. The room temperature (297 K) results confirm that the near threshold flat crack to micro-void transition previously observed in room temperature laboratory air (Figure 2) is also observed in inert vacuum environment. Additional vacuum FCG tests were performed under identical fatigue loading (K_{max} = 7.7 MPa√m) and at elevated temperature (339 K and 366 K). The elevated temperature test results and fractographic observations revealed a similar near threshold FCG transition behavior (da/dN_{trans}). The results in Figure 3a show that the FCG transitions occur at higher da/dN with elevated temperature and that the near threshold micro-void cracking was exacerbated by temperature. Similar to the laboratory air results shown in Figure 2a, all vacuum FCG rate data nearly collapse to a single temperature-independent curve ($da/dN|_{297\ K} = da/dN|_{339\ K} = da/dN|_{366\ K}$) where flat crack morphology is observed for $da/dN > (da/dN_{trans})$. The time-based transition crack growth rate, log (da/dt_{trans}), is plotted versus the reciprocal of test temperature (1/T) in Figure 3b. The linear Arrhenius behavior shown in Figure 3b suggests that a single time and temperature dependent mechanism is responsible for the near threshold micro-void crack growth behavior.

Constant ΔK FCG testing was conducted to show that the near threshold micro-void crack growth described in Figure 3 is related to a time dependent damage mechanism. Figure 4 shows the results of laboratory air FCG experiments conducted at a constant ΔK = 0.77 MPa√m and three different loading frequencies (11 Hz, 5 Hz, and 1 Hz). Testing was performed at a K_{max} = 5.5 MPa√m to ensure that crack growth was conducted within the accelerated FCG regime identified in "region-d" of Figure 2a. The plot of crack length versus load cycle (N) in Figure 4a reveals an increase in micro-void FCG rate with decreased loading frequency; here, the constant FCG rate, linear slope ($\Delta a/\Delta N$), was calculated for each loading frequency (f). Room temperature FCG rates at ΔK levels that are above the da/dN transition (flat crack morphology) shown in Figures 2 and 3 are independent of frequency [7]. Figure 4b shows the constant ΔK data plotted as crack length versus time (t), where t = (N)(f). The near linear slope shown in Figure 4b shows that the near threshold phenomenon is the result of a time dependent crack growth mechanism. Identical constant ΔK tests, not reported here, were also conducted in inert vacuum; similar time dependent crack growth behavior was observed in the UHV environment. The UHV results show that the laboratory air frequency effect was not the result of crack-tip environment interactions.

A series of static load tests were conducted to show that the near threshold micro-void crack growth phenomenon is the result of room temperature creep. Here, the test load was selected to create an initial crack-tip stress intensity factor (K = 5.5 MPa√m) that was identical to the value of K_{max} that produced micro-void crack growth during near threshold FCG testing (refer to Figure 2). No visible

crack growth was observed on the specimen surface during these constant load tests. However, because micro-void crack growth was limited to the specimen interior (crack tunneling) during constant-K_{max} fatigue testing [7], it was suspected that constant-load crack growth might also be limited to the specimen interior. To investigate the tunneled crack growth behavior, a series of tests were conducted under static load conditions with intermittent fatigue; here, intermittent fatigue loading was used to produce a characteristic fatigue crack surface that marked the regions of constant load cracking. The micrographs in Figure 5a and 5b show the fracture surface of specimen that was pre-cracked by fatigue loading at a constant ΔK = 5.5 MPa$\sqrt{m}$ (K_{max} = 11.0 MPa$\sqrt{m}$, R = 0.5 and f = 10 Hz); these test parameters resulted a relatively straight crack front (dashed line). Fatigue pre-cracking was stopped after a steady-state FCG rate was established. Following the pre-crack, a static load corresponding to the maximum fatigue load (K = 11.0 MPa$\sqrt{m}$) was maintained for a specified time. After each static load test, fatigue loading (pre-crack parameters) was resumed until steady-state FCG rate conditions were reached to (1) mark the final static load crack front (solid line in Figures 5a and 5b) and (2) reestablish a straight fatigue crack front for the next static load test. A total of eight static load tests were performed maintaining the prescribed load for different time intervals ranging from 1 hour to 120 hours. Examination of the resulting crack surface revealed a change in crack surface morphology during the static load tests. Figures 5a and 5b are micrographs that show the crack surface produced during static loading for 43 hours and 10 hours, respectively. The light colored regions bounded by the dashed line (fatigue pre-crack front) and the solid line (tunneled static load crack front) is the region of constant load cracking. Detailed SEM examinations revealed that all eight static load crack surfaces exhibited the same micro-void morphology and crack-tunneling configuration observed during near threshold FCG testing (Figure 2b). The tunneled crack configuration required for micro-void crack growth indicates that the time and temperature dependent damage mechanism is a plane-strain (triaxial state of stress) induced damage mode that is characteristic of creep crack growth. The plot of tunneled (centerline) crack length (Δa) versus test time (t) for the eight static load tests (Figure 5c) shows that room temperature creep crack growth rates are similar to the growth rate of near threshold micro-void cracking. The dashed line in Figure 5c represents the micro-void crack growth rate ($da/dt = 2.05 \times 10^{-8}$ m/s) that corresponds to the "b/c - FCG transition" in Figure 2a where early stages of micro-void (tunneled) crack growth are likely. The similar slope of the dashed line and the average creep crack growth rate (solid line) for early stages of tunneled crack growth indicate that the accelerated near threshold fatigue crack growth rates shown in Figures 2 and 3 are the result of a creep dominated crack growth mechanism.

CONCLUSIONS

Results show that the near threshold accelerated fatigue crack growth observed in aluminum alloy 8009 is the result of a creep dominated damage mechanism. The micro-void crack growth mechanism requires a high local triaxial state of stress (plane-strain specimen interior) and elevated K_{max} levels ($K_{max} > 0.4\ K_{IC}$) during fatigue loading.

The room temperature creep mechanism was only observed in the near threshold regime at elevated levels of mean stress. Consequently, the constant K_{max} test procedure was critical in identifying and characterizing the near threshold phenomenon.

REFERENCES

(1) Newman, J.C., Jr. and Elber W. (eds.), *Mechanics of Fatigue Crack Closure, ASTM STP 982*, ASTM, 1988.

(2) Gan, D. and Weertman, J., *Engineering Fracture Mechanics,* Vol. 15, 1981, pp. 87-106.

(3) Beevers, C., *Metals Science*, August/September 1977, pp. 362-367.

(4) Marci, G., *Proceedings of the 6th Int. Fatigue Conf.*, Vol. 1, 1996, pp. 493-498.

(5) Lang, M., Hartman, G. and Larsen, J., *Scripta Materialia* Vol. 38, 1998, pp. 1803-1810.

(6) Lang, M., *Acta Materialia*, Vol. 47, 1999, pp. 3247-3261.

(7) Newman, J.A., Riddell, W.T. and Piascik, R.S., *ASTM STP 1372*, ASTM, 2000, pp. 63-77.

(8) Jata, K., Maxwell, D. and Nicholas, T., *J. Engineering Mater. Tech.,* Vol. 116, 1994, pp. 45-53.

(9) Claeys, S., Jones, J., and Allison, J., *Dispersion Strengthened Aluminum Alloys*, Y.W. Kim and W.M. Griffith (eds.), 1988, pp. 323-336.

(10) ASTM, *Annual Book of ASTM Standards*, Vol. 3.01, E647, 2001.

(11) Piascik, R.S., Newman, J.C., Jr., and Underwood, J.H., *Fatigue and Fracture of Engineering Materials and Structures,* Vol. 20, 1997, pp. 559-563.

(12) Donald, J.K., Bray, G., and Bush, R., *High Cycle Fatigue of Structural Materials*, W.O. Soboyejo and T.S. Srivatsan (eds.), 1997, pp. 123-141.

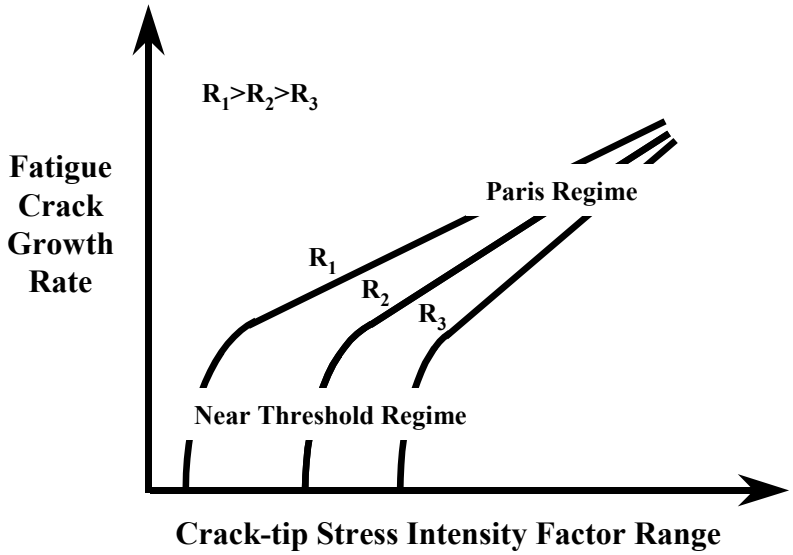

FIGURE 1 A schematic showing the fatigue crack growth threshold and Paris regime. As the stress ratio (R) is increased, a pronounced increase in fatigue crack growth rate is typically observed in the near threshold regime.

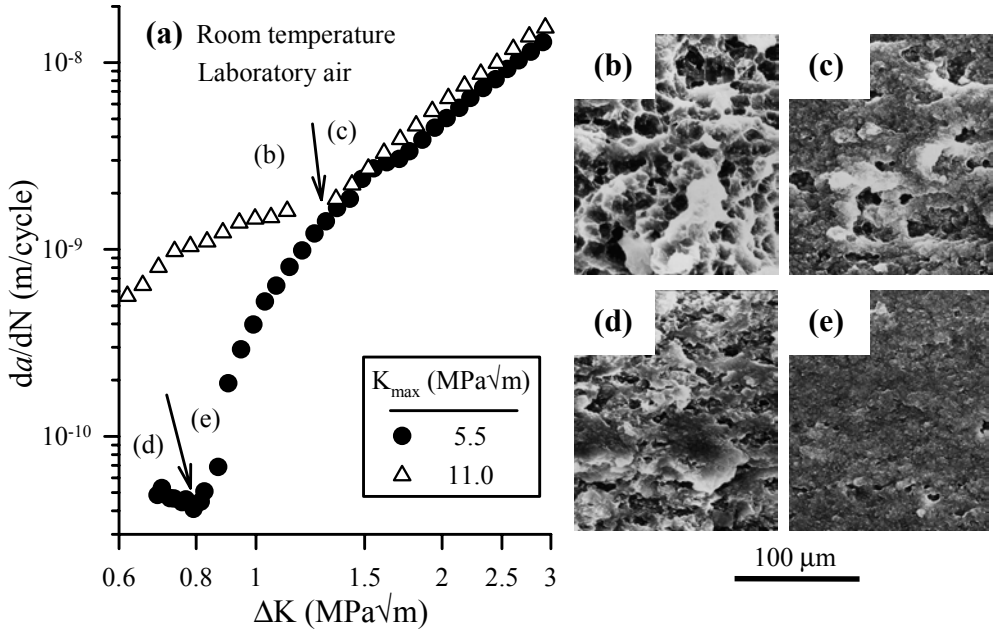

FIGURE 2 (a) Constant-K_{max} FCG data for K_{max} of 5.5 and 11.0 MPa√m (f = 10 Hz). FCG transitions (arrows) mark with changes in crack surface morphology. (b and c) Micro-void crack surface produced at K_{max} = 11.0 MPa√m and $\Delta K < 1.3$ MPa√m and a flat surface produced at $\Delta K > 1.3$ MPa√m, respectively. (d and e) Micro-void crack surface produced at K_{max} = 5.5 MPa√m and $\Delta K < 0.8$ MPa√m and a flat surface produced at $\Delta K > 0.8$ MPa√m, respectively.

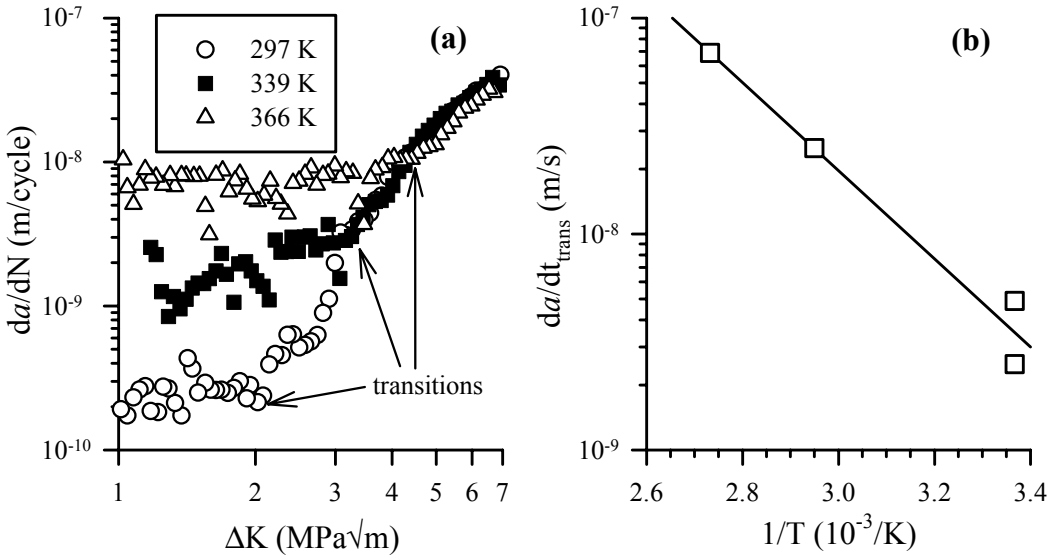

FIGURE 3 (a) Ultra high vacuum constant-K_{max} = 7.7 MPa√m FCG data (f = 10 Hz) are shown for three temperatures (297 K, 339 K, and 366 K). (b) Shown is an Arrhenius plot of transition (time dependent) crack growth (d*a*/dt) versus temperature (1/T).

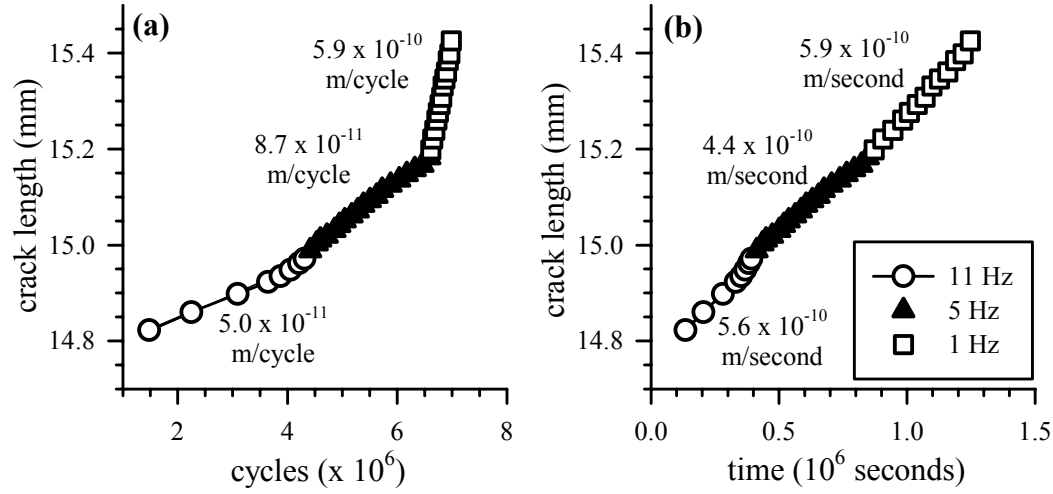

FIGURE 4 (a) Laboratory-air, room-temperature constant ΔK = 0.77 MPa√m FCG test results (K_{max} = 5.5 MPa√m) conducted at 11 Hz, 5 Hz, and 1 Hz. The change in slope shows a distinct increase in FCG rate (d*a*/dN) with decreased load frequency. The same data are plotted in (b) as crack length versus time; a constant crack growth rate (per unit time), d*a*/dt is observed.

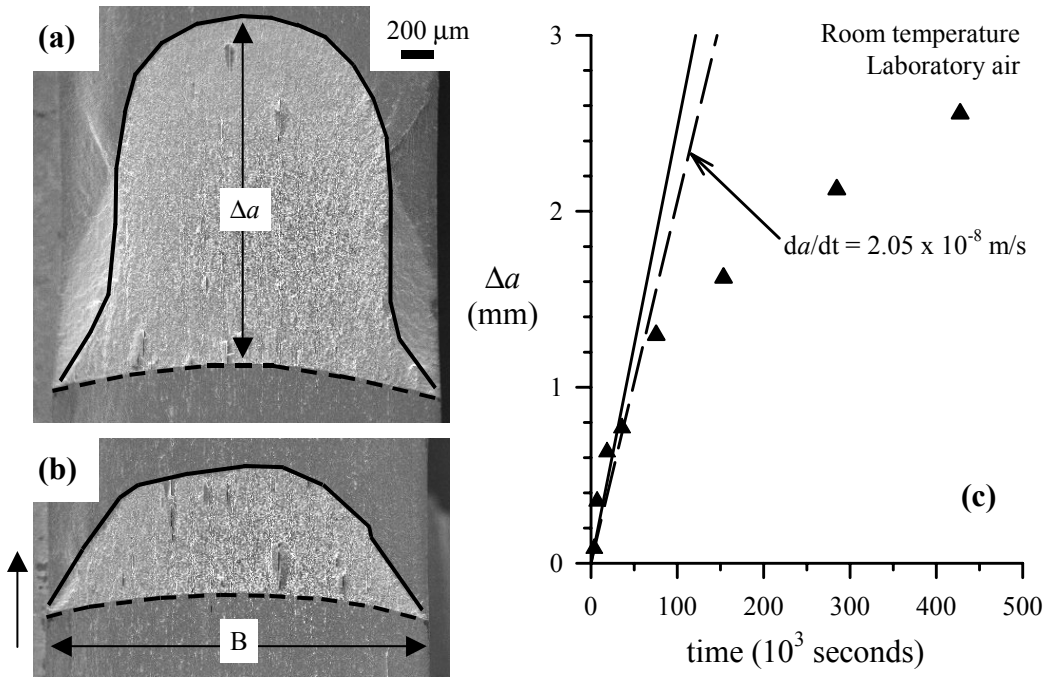

FIGURE 5 (a and b) Shown are tunneled crack surface produced by constant load time dependent crack growth during a 43-hour test and 10-hour test, respectively. The specimen thickness is "B" and direction of crack growth (arrow, ↑) is noted. (c) The plot shows crack growth at the specimen centerline, Δa, versus time for eight experiments performed at times ranging from 1 hour to 120 hours.